SPECIAL 2024 3D PRINTING NSF

Effects of Postmanufacture Conditioning on the Mechanical and Hygroscopic Properties of Extrusion Printed Wood–Sodium Silicate Composites

Adefemi A. Alade Hojat Hematabadi Robert H. R. Carne
Japneet Kukal Audrey Q. Fu Armando G. McDonald
Michael R. Maughan Ahmed A. Ibrahim Daniel J. Robertson

Abstract

Additive manufacturing of wood–sodium silicate composites could aid in mitigating the carbon footprint of the building and construction industry. However, the effect of postmanufacture conditioning on the mechanical and physical properties of additively manufactured wood–sodium silicate composites is not well understood. This study investigated eight different postmanufacture drying processes, including: ambient indoor and outdoor conditions, oven-drying at two different temperatures, microwave drying, alcohol-induced dehydration using ethanol and denatured alcohol, and desiccant drying. Each postmanufacture conditioning treatment was assessed in terms of total moisture extraction and moisture extraction rate as well as the flexural strength, flexural stiffness, and hardness of the wood–sodium silicate samples after drying. In addition, the water absorption and volumetric swelling properties of the additively manufactured wood–sodium silicate samples were assessed via water submersion tests. The postmanufacture conditioning treatments were found to significantly affect the mechanical and physical properties of the samples. A universal ranking system was established based on cumulative rankings of each evaluated characteristic. Samples dried in ambient outdoor conditions achieved the best overall ranking and had the smallest carbon footprint. However, ovendried samples had the best flexural properties. Future studies investigating hybrid approaches in which composites are sequentially subjected to different drying methods will likely provide the most desirable mechanical and physical properties of wood–sodium silicate composites.

Production processes and materials employed in the building and construction sector are responsible for nearly 40 percent of global CO_2 emissions (Ding et al. 2023). Recent environmental legislation is urging the building and construction industry to adopt more sustainable processes and materials (Rasyid et al. 2018). It was recently suggested that additive manufacturing of wood–sodium silicate composites (Bhatia and Sehgal 2023) could aid in reducing the carbon footprint of the construction industry (Carne et al. 2023, Hegab et al. 2023). Wood is one of the most widely available natural and renewable building materials and is a much greener alternative to synthetic construction materials such as steel and concrete. Wood products require less fossil fuel than nonwood alternatives, and wood is naturally composed of carbon that is pulled from the atmosphere. Some wood products have negative carbon footprints. Sodium silicate is a low-cost, environmentally friendly inorganic thermoset binder used in many composite formulations (Rasyid et al. 2018, Chai et al. 2021, Xin et al. 2023). Additive

The authors are, respectively, Postdoctoral Fellow, Dept. of Civil and Environ. Engineering (aladeadefemi@outlook.com), Graduate Research Assistant, Dept. of Civil and Environ. Engineering (hema6593@vandals.uidaho.edu), PhD Candidate, Dept. of Mechanical Engineering (carn0700@vandals.uidaho.edu), PhD Candidate, Dept. of Forest, Rangeland and Fire Sciences (kuka9993@vandals.uidaho.edu), Affiliate Professor, Dept. of Mathematics and Statistical Science (audreyf@uidaho.edu), Professor, Dept. of Forest, Rangeland and Fire Sciences (armandm@uidaho.edu), Associate Professor, Dept. of Mechanical Engineering (maughan@uidaho.edu), Associate Professor, Dept. of Civil and Environ. Engineering (aibrahim@uidaho.edu), and Associate Professor, Dept. of Mechanical Engineering (danieljr@uidaho.edu [corresponding author]), Univ. Idaho, Moscow, Idaho.
This paper was received for publication in April, 2024. Article no. 24-00018.

Forest Prod. J. 74(S1):11–21.
doi:10.13073/FPJ-D-24-00018

manufacturing of wood-based sodium silicate composites is still at a developing stage (Bhatia and Sehgal 2023) but is gaining interest due to the many advantages of timber-based additive manufacturing, which include minimal production waste, reduced embodied energy, and reduced human labor inputs (Attaran 2017, Bhatia and Sehgal 2023). The feasibility of additively manufacturing wood–sodium silicate composites has been demonstrated in studies by Orji et al. (2023) and Carne et al. (2023). However, the appearance as well as the physical and mechanical properties of additively manufactured wood–sodium silicate composites are highly influenced by postmanufacture conditioning treatments (Saroia et al. 2020). Thus far, only ambient indoor conditioning (Carne et al. 2023) and ovendrying (Orji et al. 2023) methods have been explored, with reported undesirability in the resulting mechanical and physical properties.

The impact of postmanufacture conditioning techniques on the mechanical and physical properties of additively manufactured wood–sodium silicate composites has not been explored previously. This study compared the mechanical and physical properties of additively manufactured wood–sodium silicate samples that were exposed to eight different postmanufacture conditioning processes. These drying processes included: (1) ambient indoor conditions, (2) ambient outdoor conditions, (3) oven-drying at 60°C for 72 hours, (4) oven drying at 100°C for 24 hours, (5) microwave drying, (6) alcohol-induced dehydration using ethanol, (7) alcohol-induced dehydration using denatured alcohol, and (8) desiccant drying. These processes were selected based preliminary experimentation and are commonly used methods for drying lumber. The overall goal of these investigations was to discover the effect of postmanufacture conditioning on the dimensional stability of samples, as well as the mechanical and physical characteristics of the samples.

Materials and Methods

Materials and composite formulation

Sawmill residues of mixed wood species were obtained from Plummer Forest Products (Post-Falls, Idaho). The mill residues were sieved through a 40-mesh screen to obtain wood flour with a particle size $\leq$425 μm. The moisture content of the wood flour was approximately 8 percent. Wood flour was mixed with 37 percent sodium silicate solution (Thermo Fisher Scientific, Waltham, Massachusetts) to obtain a 50 percent wood and 50 percent sodium silicate (on a dry weight basis) formulation as described by Orji et al. (2023) and Carne et al. (2023).

Extrusion printing of wood–sodium silicate composite

The wood–sodium silicate mix was fed into the extrusion printing system described in Carne et al. (2023) and shown in Figure 1. The input hopper was equipped with an agitator, and the mix was fed into the single-screw extruder at a rate of 47 g/min. A flexible polytetrafluoroethylene chemical hose with stainless-steel braided reinforcement connected the barrel of the screw extruder to a print nozzle, which was attached to an *x*-*y* positioning stage. Printing parameters used in this study are displayed in Table 1. Strips of extrusion-printed wood–sodium silicate composite were produced that measured 850 mm long by 35 ± 5 mm wide by 15 ± 2 mm high. In total, 40 test samples measuring 250 mm in length were then cut from these strips. The test samples were randomly distributed into eight groups with each group containing five test samples. Each group was then randomly assigned to one of the eight postmanufacture conditioning procedures investigated in this study.

Moisture content and extracted moisture calculations

Equations 1 and 2 were used to determine the moisture content of samples and to calculate the moisture extracted during postmanufacture conditioning, where: wet mass was determined by weighing the samples immediately after they had been manufactured, and the mass after conditioning was determined by weighing the samples after being subjected to one of the eight postmanufacture conditioning procedures investigated in this study. Finally, the ovendry mass was determined by oven-drying the samples at 105°C for 24 hours.

$$\begin{aligned} &\textit{Moisture Content}\,(\%),\ \textit{wet basis} \\ &= \frac{\textit{Wet mass} - \textit{Ovendry mass}}{\textit{Wet mass}} \times 100 \end{aligned} \tag{1}$$

$$\begin{aligned} &\textit{Extracted Moisture}\,(\%),\ \textit{wet basis} \\ &= \frac{\textit{Wet mass} - \textit{Mass after conditioning}}{\textit{Wet mass}} \times 100 \end{aligned} \tag{2}$$

The duration of each postmanufacture conditioning treatment was determined by conducting preliminary testing of extrusion-printed sodium silicate samples. During these preliminary tests, the samples were repeatedly weighed until approximately 75 percent of the moisture had been extracted from the sample or until the moisture extraction rate approached 0. The amount of time to achieve approximately 75 percent extracted moisture was then set as the duration for subsequent testing of postmanufacture conditioning treatments.

Postmanufacture conditioning in ambient indoor and outdoor environments

One group of test samples ($n = 5$) was subjected to an ambient indoor environment, while a second group of samples ($n = 5$) was subjected to an ambient outdoor conditioning. The test samples (both indoor and outdoor) were kept on wire racks for 28 days. The outdoor-dried samples were exposed to sun radiation during the months of July and August in Moscow, Idaho, but were kept away from rain showers to avoid repeated wetting cycles of the samples. The mean temperatures and humidities were 19.8°C and 46.9 percent for ambient indoor conditions and 23.1°C and 38.7 percent for ambient outdoor conditions, respectively.

Postmanufacture conditioning at elevated temperatures

One group of test samples ($n = 5$) was conditioned in an oven at 60°C for 72 hours, while a second group of test samples ($n = 5$) was conditioned at 100°C for 24 hours. At the

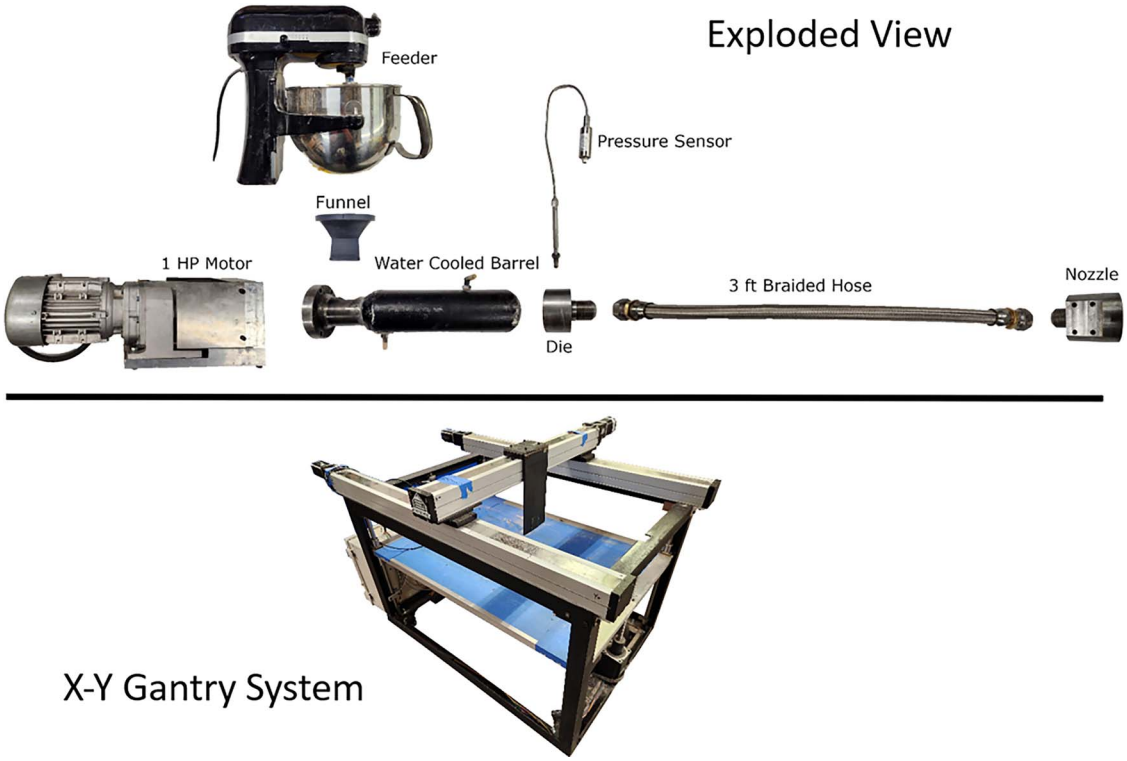

Figure 1.—Top Panel: Exploded view of extrusion printing system for wood–sodium silicate composites. Material was fed through the funnel into the screw extrusion system, where it was forced through a die and a flexible hose, which was connected to the printer nozzle. Bottom Panel: The printer nozzle was attached to an X-Y gantry system, which was suspended above a printer table that could move in the Z direction.

end of the heating cycles, the ovens were turned off, and the samples were left to gradually cool in the oven to ~36°C. Samples were then placed in a desiccator until they cooled to room temperature. This procedure was followed because rapid cooling of the samples results in bowing (see Figure 2), and samples can readily adsorb moisture from the air when at elevated temperatures (i.e., ~36°C).

Postmanufacture conditioning via microwaves

One group of test samples ($n = 5$) was conditioned using a domestic turntable microwave oven with the microwave emitter set to a power of 0.29 kW. Samples were microwaved in a cyclic manner wherein the exposure time was gradually reduced as the moisture content of the samples decreased. The maximum exposure time for a single microwave treatment was 2 minutes. After each microwave treatment the sample was allowed to cool for 5 to 10 minutes. In total, each sample was subjected to 29 minutes and 40 seconds of microwave radiation. An infrared thermal camera (FLIR model TG297) was used to measure the surface temperature of samples. The maximum temperature readings were 126°C and 122°C, on the top and bottom surface of the samples, respectively. Preliminary testing revealed that if samples were microwaved for more than 2 minutes, then the surface of the samples would develop a char layer.

Table 1.—Printing parameters for additively manufactured wood–sodium silicate samples.

Printing parameter	Value
Barrel temperature	23.1°C
Nozzle temperature	20–22°C
Fiber to resin ratio	50:50
Barrel diameter	35 mm
Die diameter	22 mm
Screw compression ratio	1:1
Screw speed	40 RPM
Extrudate velocity	179 mm/min
Volume flow rate	2.3×10^{-5} m^3/min
Print head travel speed	85 mm/min
Standoff height	15 mm

Postmanufacture conditioning via alcohol-induced dehydration

One group of test samples ($n = 5$) was subjected to alcohol-induced dehydration by submerging the sample in ethanol for 24 hours. A second group of test samples ($n = 5$) was subjected to alcohol-induced dehydration by submerging the sample in denatured alcohol for 24 hours. After the dehydration period, the samples were kept in ambient outdoor conditions of around 23.7°C and 42 percent relative humidity for 72 hours to allow the ethanol/denatured alcohol to evaporate.

Postmanufacture conditioning via desiccant-induced dehydration

One group of test samples ($n = 5$) was conditioned in a desiccator furnished with 0.9 kg of silica gel for 21 days. Anytime the silica gel in the desiccator neared its saturation, it was replaced with fresh dehydrated silica gel.

Figure 2.—Geometric distortions induced from rapid cooling of extrusion-printed wood–sodium silicate samples.

Effect of postmanufacture conditioning on mechanical and hygroscopic properties

The effects of each postmanufacture conditioning procedure on mechanical and hygroscopic properties of the extrusion-printed wood–sodium silicate composite samples were evaluated. Flexural testing, hardness testing, water absorption, and a volumetric swelling test were conducted. The test protocols for each of these methods are explained below.

Flexural testing.—Conditioned test samples were subjected to three-point bending (Figure 3) with a test span of 198 mm and test speed of 2 mm/min. The flexural test was performed using a 50-kN capacity INSTRON universal testing machine model 34TM-50 equipped with INSTRON Bluehill universal software (Figure 3). The flexural strength and modulus of elasticity were calculated from the force-displacement response of each sample. Five samples from each of the eight postmanufacture conditioning treatments were tested.

Hardness testing.—Janka ball hardness tests were conducted on the same samples used for flexural testing. Hardness tests were conducted at least 20 mm away from the loading point and the support points used during flexural testing. ASTM D1037-12 (ASTM 2012) prescribes an 11.3-mm ball diameter for modified Janka ball hardness tests. However, when employing this method, cracks were produced that propagated across the entire cross section of the test specimens. Consequently, a smaller diameter ball of 5.6 mm was manufactured and displaced at 1.5 mm/min to avoid cracking the specimens during the hardness testing. The load in pounds that drove half of the ball diameter into the specimen was recorded for each sample. Unfortunately, some specimens were destroyed during initial hardness testing attempts. Therefore, the number of successful hardness tests completed for each postmanufacture conditioning procedure varied from a minimum of four to a maximum of seven.

Water absorption and swelling tests.—Three test specimens from each postmanufacture conditioning treatment were subjected to a two-stage water absorption test as described in ASTM (2012). After samples were submerged in water for 2 hours, several parameters of interest were measured and recorded. Subsequently, the samples were resubmerged for 16 hours. Originally, the submersion period was intended to be 22 hours as is prescribed by ASTM (2012). However, several samples disintegrated after 16 hours. Therefore, all tests were stopped at 16 hours to enable accurate comparisons between groups. At the end of each submersion period, the water absorption, volumetric swelling, and swelling coefficients of the test samples were estimated using Equations 3, 4, and 5, respectively.

Figure 3.—Three-point flexure test setup.

$$\text{Water Absorption (\%), dry basis} = \frac{\text{Saturated mass} - \text{Dry mass}}{\text{Dry mass}} \times 100 \quad (3)$$

$$\text{Volumetric Swelling (\%), dry basis} = \frac{\text{Saturated volume} - \text{Dry volume}}{\text{Dry volume}} \times 100 \quad (4)$$

$$\text{Swelling Coefficient (\%), dry basis} = \frac{\text{Saturated dimension} - \text{Dry dimension}}{\text{Dry dimension}} \times 100 \quad (5)$$

Dimensions in Equation 5 represent length, thickness, and width for length, thickness, and width swelling coefficients, respectively.

Effect of postmanufacture conditioning on sample chemistry

The effect of postmanufacture conditioning on sample chemistry was investigated via Fourier transform infrared (FTIR) spectroscopy. Portions of samples from each postmanufacture conditioning treatment were mixed, ground, homogenized, and ball-milled into powders. FTIR spectra of the ground powder were then collected using a Thermo Scientific Nicolet iS10 FTIR spectrometer with a 4,000 to 650 cm^{-1} range with an attenuated total reflectance diamond accessory and an 8 cm^{-1} resolution. Background scans were performed before collecting the spectrum for each sample. OMNIC Specta software version 2.2.43 was used to perform qualitative analyses of all sample spectra, which involved baseline correction, adaptive smoothing for spectral noise reduction in regions without

peaks, and normalization to 1 absorbance unit with the highest peak in the full spectral range as basis.

Statistical analyses

Analysis of covariance (ANCOVA) tests were employed to quantify the effects postmanufacture conditioning treatments on mechanical, hygroscopic, and chemical properties of extrusion-printed wood–sodium silicate samples. ANCOVA performs linear regression with the treatments and covariates as the explanatory variables, assuming a normal distribution for the response variable with a constant variance, as well as linear relationships between each explanatory variable and the response. Sample thickness, sample width, and sample density were treated as covariates. Linearity assumptions were validated by checking pairwise scatterplots of the data. The normality assumption was checked using quantile-quantile (Q-Q) plots of the residuals from the regression. The homoscedasticity assumption was validated by checking the scatterplot of residuals versus predicted values from the fitted model of each response variable. Assumptions of homogeneity of regression slopes (i.e., independence of assigned covariate[s] and drying method) were validated by observing no significant interaction between covariate(s) and postmanufacture conditioning treatment in the fitted linear model. Statistical analyses were further performed on data with outliers included and with outliers excluded to examine sensitivity of the results to outliers. In all cases, the level of statistical significance of the coefficients remained unchanged with and without outliers, indicating robustness of the inference results. Therefore, the results presented in this article were derived using all the data (outliers included). More details regarding statistical testing and validity of assumptions can be found in the Supplemental information. Following ANCOVA tests, post hoc analyses were performed based on estimated marginal means (emmeans), also known as the predicted means of the treatments. The Benjamin-Hochberg method for controlling the false discovery rate (FDR) was employed to account for multiple pairwise comparisons to control the overall errors. All statistical analyses were performed using R programming in RStudio version 2023.06.1.0, Build 524 (Posit PBC).

Results and Discussion

Effects of postmanufacture conditioning on moisture extraction

The moisture content of extrusion-printed wood–sodium silicate composite samples was 43.50 percent on a wet basis at the time of manufacture. As expected, samples that underwent either the oven or microwave postmanufacture conditioning treatments demonstrated the highest extracted moisture percent. In addition, the microwave treatment demonstrated the highest moisture extraction rate (i.e., mean extracted moisture percentage as a function of time). Figure 4 summarizes the extracted moisture percent and the moisture extraction rate for each of the postmanufacture conditioning treatments.

As noted previously, the thickness of extrusion-printed sodium silicate samples varied by ±5 mm while the width varied by ±2 mm. Consequently, width and thickness were assigned as covariates during ANCOVA testing. The ANCOVA analysis revealed that thickness had a significant effect ($p < 0.05$) on moisture extraction percent and moisture extraction rate. However, the effect of width was not found to be statistically significant. As expected, postmanufacture conditioning treatment had a significant effect on extracted moisture percentage ($p < 0.05$) with a size effect of 0.968. All ANCOVA results can be found in Supplemental Figures S1 to S4 and Supplemental Tables S1 and S2.

Effects of postmanufacture conditioning on flexural strength

The mean flexural strength of extrusion-printed wood–sodium silicate composite samples varied from 7.56 to 19.1 MPa. The ethanol-induced dehydration samples recorded the lowest mean flexural strength, while samples oven-dried at 60°C for 72 hours had the highest mean flexural strength (Figure 5). During ANCOVA testing, the density of test samples was assigned as a covariate. As expected, the effect of postmanufacture conditioning treatment on flexural strengths was statistically significant ($p < 0.05$) with an effect size of 0.835. Complete ANCOVA results are reported in Supplemental Figures S5 to S7 and Supplemental Tables S3 and S4. Microwaved samples demonstrated internal voids and cracks as

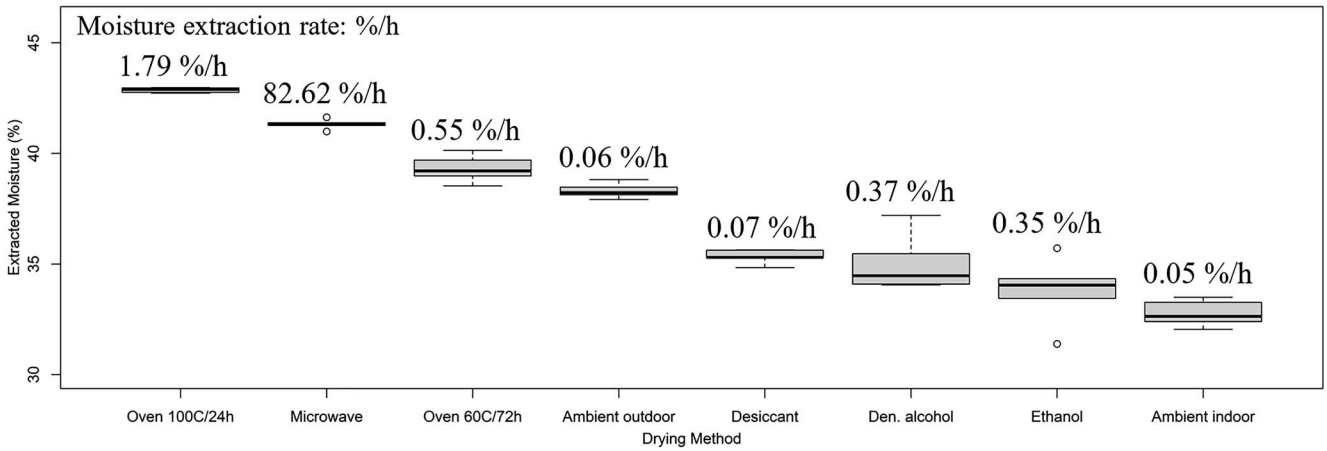

Figure 4.—Box plots of extracted moisture percentage of extrusion-printed wood–sodium silicate samples for each postmanufacture drying method with moisture extraction rates displayed as inset values.

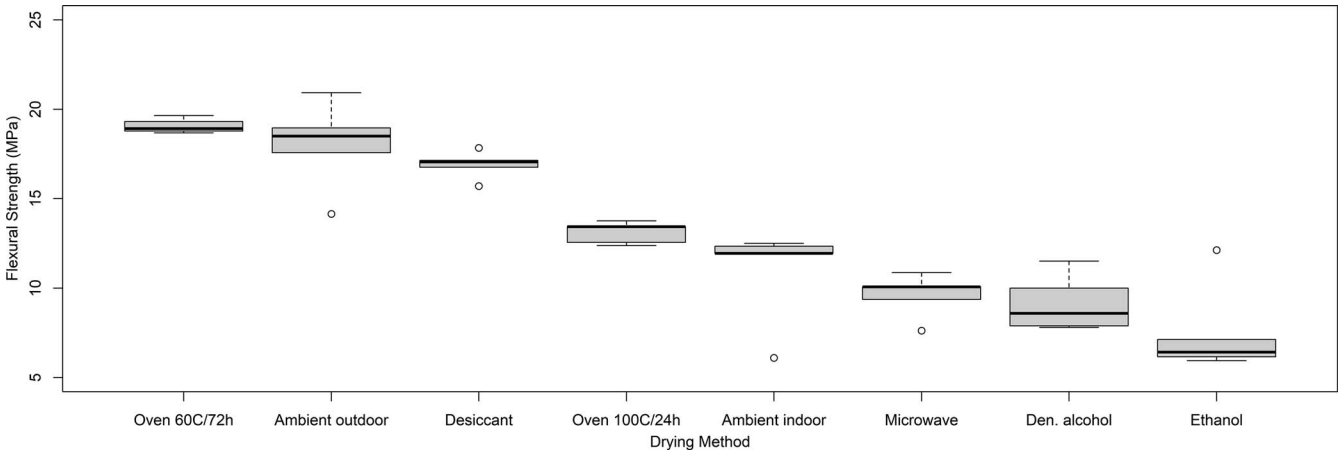

Figure 5.—Box plots of flexural strength of extrusion-printed wood–sodium silicate samples for each postmanufacture conditioning treatment.

shown in Figure 6. Voids and cracks such as these adversely affect flexural strength.

Effects of postmanufacture conditioning on flexural modulus of elasticity

The mean flexural modulus of elasticity of extrusion-printed wood–sodium silicate composite samples varied from 1,488 to 4,099 MPa. In general samples with the highest and lowest flexural strengths also demonstrated the highest and lowest flexural moduli of elasticity. Overall, ethanol-dehydrated samples recorded the lowest mean flexural modulus of elasticity, while samples oven-dried at 60°C for 72 hours had the highest mean flexural modulus of elasticity (Figure 7). Sample density was treated as a covariate during ANCOVA testing. The effect of postmanufacture conditioning treatment on flexural modulus of elasticity was statistically significant ($p < 0.05$) with a size effect of 0.899. Full details of ANCOVA testing results, assumptions, and post hoc analyses are presented in Supplemental Figures S8 to S10 and Supplemental Tables S5 and S6.

Effects of postmanufacture conditioning on sample hardness

The mean hardness of test samples varied from 1,330 to 3,340 N. Interestingly, the observed trend in flexural properties did not correlate with the observed trend in hardness of the samples. In particular, the microwaved samples recorded the lowest mean hardness, followed by samples oven-dried at 100°C for 24 hours (see Figure 8). Samples dried in a desiccator had the highest mean hardness, followed by samples subjected to ambient outdoor conditions (Figure 8). ANCOVA results are presented in Supplemental Figures S11 to S13 and Supplemental Tables S7 and S8. The effect of postmanufacture conditioning treatment on sample hardness was statistically significant ($p < 0.05$) with an effect size of 0.639.

Effects of postmanufacture conditioning on water absorption characteristics

At the end of the initial 2-hour water submersion test, only those samples subjected to ambient outdoor conditions,

Figure 6.—Internal cracks and voids formed following microwave-induced curing of extrusion-printed wood–sodium silicate samples.

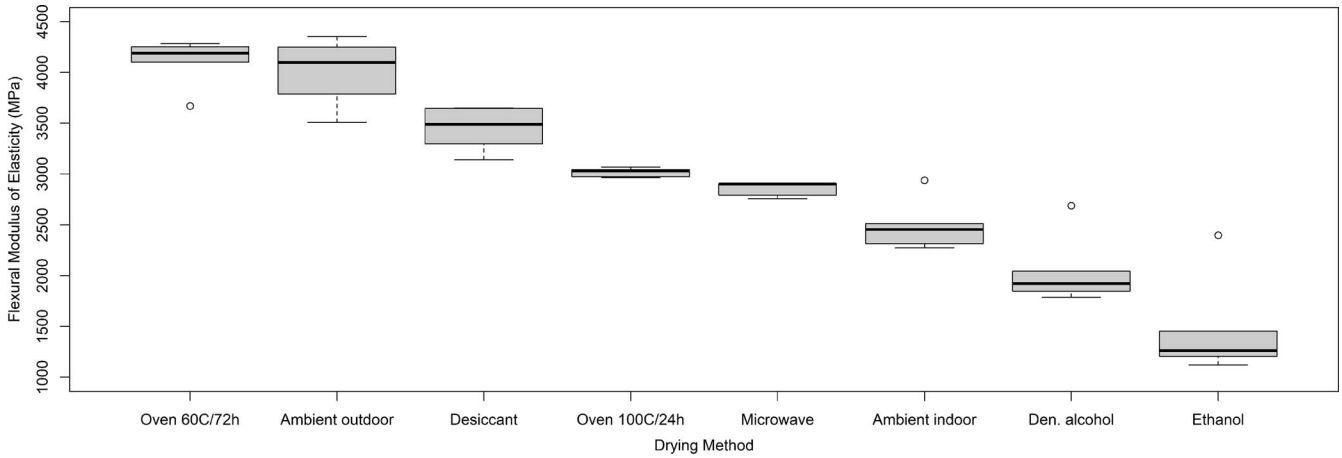

Figure 7.—Box plots of flexural moduli of elasticity of extrusion-printed wood–sodium silicate samples for each postmanufacture conditioning treatment.

microwave radiation, or oven-drying at 100°C for 24 hours showed no sign of disintegration. Samples subjected to ambient indoor conditions completely disintegrated after 2 hours. The samples dried in a desiccator and those subjected to ethanol- and denatured alcohol–induced dehydrations exhibited moderate to severe disintegration, while samples dried in an oven at 60°C for 72 hours exhibited moderate to slight disintegration. The water absorption percentages following 2 hours of water submersion are presented in Supplemental Figure S14. Surprisingly, the ambient outdoor-dried samples exhibited lower water uptake after 2 hours of submersion as compared to samples dried in an oven at 100°C for 24 hours and microwave-dried samples. In particular, samples dried in ambient outdoor conditions, in an oven at 100°C, and by microwave radiation recorded mean water absorptions of 46.0 percent, 74.6 percent, and 81.3 percent, respectively. After the subsequent 16-hour submersion test, all of the samples completely disintegrated except for those that were dried in a microwave or oven at 100°C for 24 hours. The mean water absorptions after the 16-hour test were 94.6 percent for microwave-dried samples and 98.4 percent for samples oven-dried at 100°C.

Effects of postmanufacture conditioning on volumetric swelling characteristics

The volumetric, longitudinal (length), thickness, and width swelling percentages at the end of the initial 2-hour water submersion test are presented in Supplemental Figures S15 to S18. Samples dried in ambient outdoor conditions, in an oven at 100°C for 24 hours, and in a microwave demonstrated mean volumetric swelling of 17.6 percent, 28.2 percent, and 25.2 percent, respectively, mean longitudinal swelling of 1.60 percent, 4.18 percent, and 4.33 percent, respectively, mean thickness swelling of 12.4 percent, 16.9 percent, and 15.3 percent, respectively, and mean width swelling of 2.92 percent, 5.29 percent, and 4.07 percent, respectively. The ambient outdoor-dried samples exhibited better short-term swelling performance as compared to samples dried in an oven at 100°C or dried in a microwave. After the 16-hour submersion test, the microwave-dried samples demonstrated slightly lower mean volumetric swelling (36.1%) than samples dried in oven at 100°C for 24 hours (39.1%). The longitudinal, thickness, and width swelling for microwave-dried samples and samples oven-dried at 100°C for 24 hours were comparable with the former recordings from the 2-hour submersion

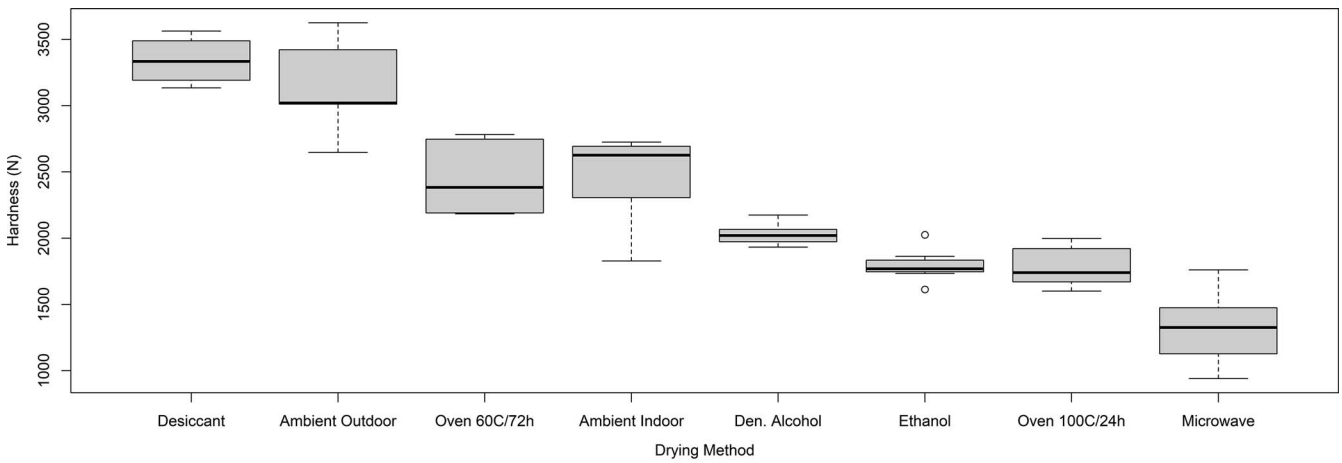

Figure 8.—Box plot for hardness of extrusion-printed wood–sodium silicate samples for each postmanufacture conditioning treatment.

test. In general, all samples demonstrated more swelling in thickness than in length or width.

Effects of postmanufacture conditioning on sample chemistry

Postmanufacture conditioning treatment did not appear to have a large effect on sample chemistry. In general, the spectra of the extrusion-printed wood–sodium silicate samples exhibited FTIR spectra band intensity reduction and a few band disappearances. Figure 9 shows the FTIR spectra associated with each postmanufacture conditioning treatment as well as the FTIR spectra of untreated wood flour. Band disappearance and reduced intensities at the tail end of the fingerprint region (897 cm^{-1} to 558 cm^{-1}) differentiated the extrusion-printed wood–sodium silicate sample chemistry from the control (wood). The intensities of other bands investigated in this study are shown in Table 2. The reductions in band intensities at 3,330, 1,729, 1,637, 1,314, 1,262, 1,157, 1,103, and 1,027 cm^{-1} were attributable to moisture extraction from the wood–sodium silicate samples. Samples subjected to oven-drying at 100°C and microwave drying had the lowest polar functional group intensity, while samples subjected to ethanol-induced dehydration and ambient indoor conditioning had the highest polar functional group band intensity.

Ranking of postmanufacture conditioning treatments

An ideal postmanufacture conditioning treatment would render extrusion-printed wood–sodium silicate composites impervious to moisture and enhance material properties while requiring minimal energy expenditure and time. As expected, none of the investigated drying methods was able to achieve all these ideals. Therefore, each postmanufacturing conditioning treatment was assigned a rank for each of the characteristics evaluated in this study (see Table 3). The rankings were based on the magnitude of each acquired measurement and statistical differences between conditioning treatments obtained from ANCOVA tests. A universal ranking categorization (A to G) was assigned based on the cumulative rankings of each characteristic evaluated in the study. Ambient outdoor conditioning provided the most desirable characteristics, while ethanol-induced dehydration provided the least desirable overall characteristics (Table 3). It is interesting to note that ambient outdoor conditioning not only produced the most desirable characteristics, but it would also be the most economically advantageous postmanufacture conditioning treatment as it requires no added energy or chemicals. In a future study, it would be beneficial to conduct a full techno-economic analysis of promising postmanufacturing conditioning treatments. We believe ambient drying may have produced the best mechanical and physical

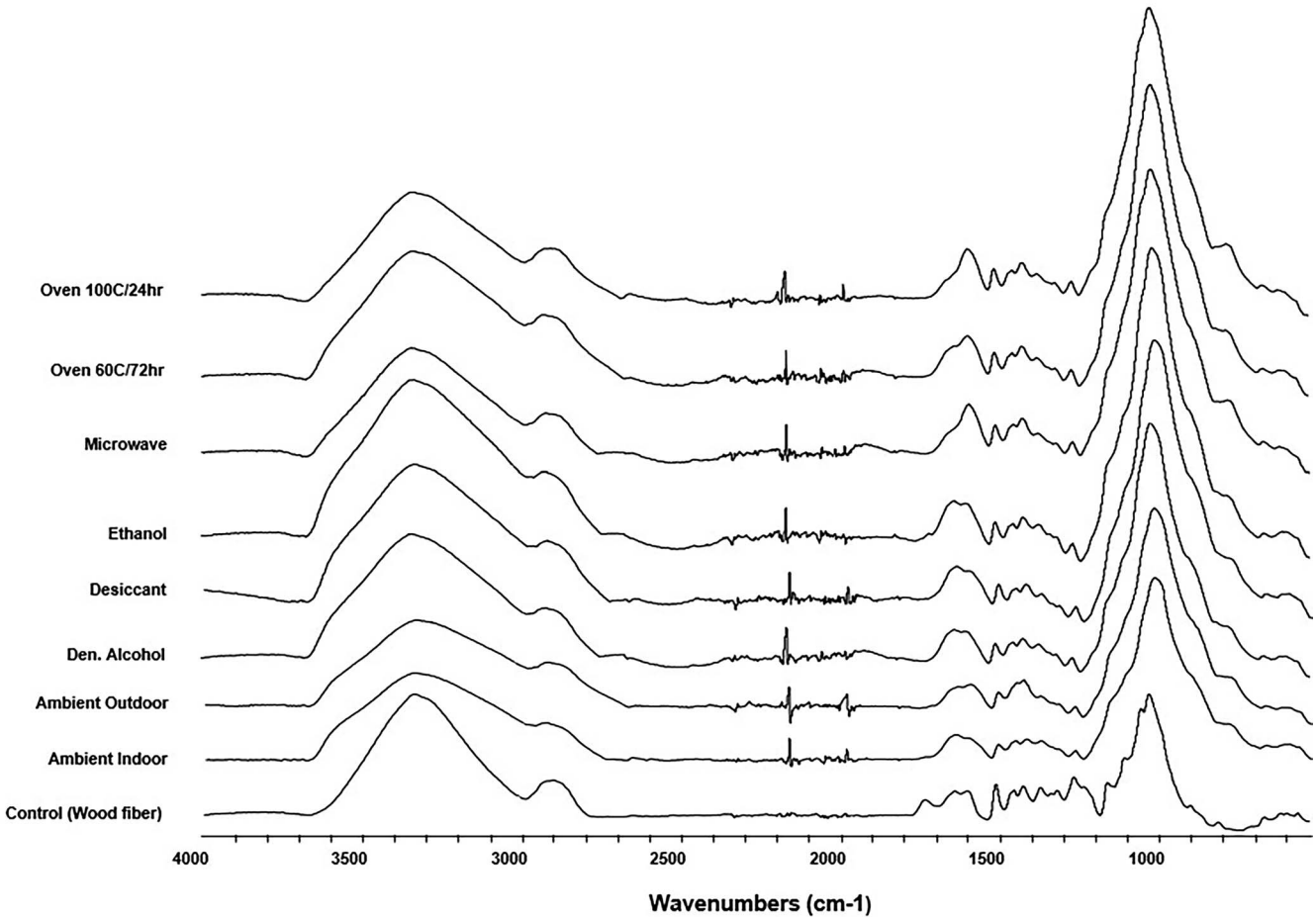

Figure 9.—FTIR spectra of control (wood flour) and dried wood–sodium silicate samples from different postmanufacture drying methods.

Table 2.—Wood–sodium silicate composite band assignments (Alade et al. 2023).

Frequency	Group
3,330 cm^{-1}	Hydroxyl group (O–H stretching)
1,729 cm^{-1}	Carbonyl group (C=O stretching)
1,637 cm^{-1}	Delta-bonded water molecules (H–O–H)
1,510 cm^{-1}	Aromatic skeletal vibrations in lignin
1,450 cm^{-1}	CH_2, C–H deformation in lignin and carbohydrates
1,421 cm^{-1}	CH_3, C–H deformation in lignin and carbohydrates
1,367 cm^{-1}	(CH)–(CH_3), C–H deformation in cellulose and hemicellulose (Pandey and Pitman 2003, Lai and Idris 2013, Alade et al. 2023)
1,314 cm^{-1}	C–O stretching
1,262 cm^{-1}	C–O stretching
1,157 cm^{-1}	Asymmetric vibration of C–O–C
1,103 cm^{-1}	C–O and O–H vibrations
1,027 cm^{-1}	Symmetric vibration of (C–O–C)

properties because the drying rate was more gradual, which may have resulted in less drastic moisture differences through the thickness of the sample. This in turn would result in less separation and creation of small internal voids due to shrinking and swelling.

Sequentially subjecting samples to multiple postmanufacturing conditioning treatments may ultimately provide the most desirable characteristics of extrusion-printed wood–sodium silicate composites. For example, a hybrid postmanufacture drying method starting with ambient outdoor drying followed by heating at 100°C or microwave drying may be particularly effective. Ambient outdoor drying produces desirable mechanical properties and requires little energy investiture. The ambient outdoor conditioning could be used to drive off most of the sample's moisture, after which the samples could be oven dried at 100°C or microwaved to enable a more complete curing reaction to take place between wood and sodium silicate. The more complete curing provided by oven-drying or microwaving would in turn provide better water absorption characteristics and dimensional stability of the composite.

Several of the conditioning treatments investigated are suitable for drying wood–sodium silicate composites that become damp during their service life (e.g., due to water leaks, flooding, or humidity changes). Microwave and desiccant-based drying units are currently employed in the construction industry to regulate moisture and could readily be applied to building components made of extrusion-printed wood–sodium silicate composites. However, further research into microwave drying still needs to be conducted. In particular, reducing the microwave drying cycle and increasing the time between cycles would allow for more uniform moisture removal (Novotný et al. 2014) and therefore avoid creation of internal cracks and voids in the composite.

Comparison to 3D-printed concrete

Limitations.—Extrusion-printed wood–sodium silicate composites have been suggested as a potential alternative to 3D-printed concrete (Carne et al. 2023). Table 4 provides comparisons between additively manufactured wood–sodium silicate composites and 3D-printed concrete products. The flexural properties of wood–sodium silicate composites are generally better than those of 3D-printed concrete products. However, improvements in the water repellency and weathering resistance of wood–sodium silicate composites are critical to achieving viable construction products. Consequently, there is a great need to explore the effects of additives and/or coatings on the water absorption and weatherability characteristics of additively manufactured wood–sodium silicate composites. It should be noted that such research will likely yield fruitful results because several commercially available sodium silicate-based products are used for waterproofing concrete and masonry work.

The wood species used to manufacture extrusion-printed wood–sodium silicate composites is expected to have some effect on mechanical properties. To limit the potential cofounding effects of wood species on results, all samples utilized in this study were made from the same single batch of mixed-woodspecies sawmill residues. The study design was also comparative in nature (i.e., postmanufacturing conditioning treatments were directly compared to one another). Thus, while we expect wood species may affect overall mechanical properties, we do not believe the overall conclusions of this study would be altered by wood species. However, future studies directly investigating the effect of wood species on mechanical properties may be warranted. In addition, the effect of heterogeneous materials on the overall response of extrusion-printed wood–sodium silicate composites should be investigated in the future. The particle size of the sifted sawmill residues used in this study was an order of magnitude smaller than the dimensions of the test samples. Thus, a continuum assumption was made, and the test samples were treated as a single, homogeneous composite material. In addition, multiple replicates of each treatment were tested to limit any confounding effects of inhomogeneous material properties. However, if smaller test samples are used in the

Table 3.—Postmanufacture conditioning treatment rankings.

Drying method	Extracted moisture	Flexural strength	Flexural modulus	Hardness	Water absorption	Dimensional stability	Overall ranking[a]
Ambient outdoor	4	1	1	1	2	2	A
Oven 100°C/24 h	2	2	3	3	1	1	B
Oven 60°C/72 h	3	1	1	2	3	3	C
Microwave	1	4	4	4	1	1	D
Desiccant	5	1	2	1	4	4	E
Ambient indoor	6	3	5	2	5	5	F
Denatured alcohol	5	4	6	3	4	4	F
Ethanol	5	5	7	3	4	4	G

[a] Rank 1 and rank A denote best performance; rank 7 and rank G denote worst performance.

Table 4.—Comparative summary of wood–sodium silicate composite properties with 3D-printed concrete products.

Product [reference]	Postmanufacture conditioning	Mechanical properties		
		Flexural strength[a] (MPa)	Flexural MOE[ab] (MPa)	Hardness[a] (N)
Wood–sodium silicate composites [this study]	Refer to Table 3	7.59–19.1	1,488–4,099	1,326–3,340
Wood–sodium silicate composites (Carne et al. 2023)	Ambient lab conditions for 14 days	7.23–10.5	1,133–2,266	—[c]
Polyethylene (PE) fiber-reinforced concrete (Alchaar and Al-Tamimi 2021)	Ambient lab conditions for 7 days	6.19	—	—
	Outdoor at 40°C to 45°C for 7 days	7.50	—	—
Concrete with varied constituent mix ratios (Zahabizadeh et al. 2021)	Ambient indoor ranging from 3 to 28 days	>3 to <7.5	—	—
Concrete with different aggregate combinations (Xiao et al. 2022)	Air cured at ≈ 24°C to 31°C for 28 days	2.2–6.0	—	—
Concretes with natural and recycled sand (Ding et al. 2020a)	20°C ± 2°C + 95% ± 5% RH[b] from 7 to 28 days	1.2–4.5	—	—
PE fiber-reinforced concretes (Ding et al. 2020b)	20°C ± 2°C + 95% ± 5% RH[b] for 28 days	3.53–12.3	—	—
Cementitious powder (Feng et al. 2015)	Oven at 60°C for 3 h	4.12	—	—

Product [reference]	Postmanufacture conditioning	Hygroscopic properties	
		Total submersion period (h)	Water absorption (%)
Wood–sodium silicate composites [This study]	Refer to Table 3	18	94.6%–disintegration
Geopolymer concrete with different compositions (Jaji et al. 2023)	23°C ± 2°C + 65% ± 5% RH[b] for 28 days + 85°C for 24 h	24	7.32–8.26
	23°C ± 2°C + 65% ± 5% RH[b] for 90 days + 85°C for 24 h	24	6.70–7.33

[a] Perpendicular to print direction.
[b] MOE = modulus of elasticity; RH = relative humidity.
[c] — = not available.

future, a continuum assumption may not be appropriate, and it may become necessary to the treat the sample as a heterogeneous material.

Infrared drying is commonly used in multiple industries, including the construction industry (e.g., to rapidly dry paint and drywall), but this drying method was not investigated in this study. It is unclear how evenly infrared radiation would heat additively manufactured wood–sodium silicate composites or how far into the material the infrared radiation would penetrate. This should be investigated in future studies. It may be possible to add an infrared heater directly to the print head, which could dry the material immediately after leaving the print nozzle.

Table 3 list the mechanical properties of dried wood–sodium silicate composites. It should be noted that the material properties of wet or freshly printed wood–sodium silicate composite were not evaluated in this study. Immediately after the wood–sodium silicate composite has been extruded, it has the consistency of modeling clay and cannot support significant tensile or flexural loads until it has dried. However, it can withstand compressive loads due to self-weight/gravity. In other words, with the current setup, overhanging features cannot be printed without support. Attaching an infrared heater directly to the print head may enable printing of unsupported overhangs because the material could be partially cured before the weight of additional layers is added.

When deciding upon a microwave-drying procedure, no firm guidelines regarding microwave intensity or duration could be found. During preliminary testing, we noted the sample would become charred if the duration was too long or the intensity of the microwave was too high. This led to development of the microwaving procedure detailed in the "Methods" section. However, we still observed interior voids in the microwaved samples in this study (likely due to water being vaporized in the interior of the sample). As such, the microwave-induced drying procedure utilized in this study demonstrates room for significant improvement. Microwave drying may prove to be viable in future studies, but much more research is needed to fully understand the interacting effects of sample moisture, sample size, microwave duration, and microwave intensity.

Acknowledgments

The authors would like to acknowledge the National Science Foundation for funding to support this work under grant number 2119809.

Literature Cited

Alade, A. A., Z. Naghizadeh, C. B. Wessels, H. Stolze, and H. Militz. 2023. Characterizing surface adhesion-related chemical properties of copper azole and disodium octaborate tetrahydrate-impregnated Eucalyptus grandis wood. *J. Adhes. Sci. Technol*. 37(15):2261–2284. https://doi.org/10.1080/01694243.2022.2125208

Alchaar, A. S., and A. K. Al-Tamimi. 2021. Mechanical properties of 3D printed concrete in hot temperatures. *Constr. Build. Mater*. 266:120991. https://doi.org/10.1016/j.conbuildmat.2020.120991

ASTM Standard D1037, 2012, "Standard Test Methods for Evaluating Properties of Wood-Base Fiber and Particle Panel Materials" ASTM International, West Conshohocken, PA, 2012. https://doi.org/10.1520/D1037-12, www.astm.org.

Attaran, M. 2017. The rise of 3-D printing: The advantages of additive manufacturing over traditional manufacturing. *Bus. Horiz*. 60(5):677–688. https://doi.org/10.1016/j.bushor.2017.05.011

Bergman, R., M. Puettmann, A. Taylor, and K. E. Skog. 2014. The carbon impact of wood products. *Forest Prod. J*. 64(7–8):220–231. https://doi.org/10.13073/FPJ-D-14-00047

Bhatia, A., and A. K. Sehgal. 2023. Additive manufacturing materials, methods and applications: A review. *Mater. Today: Proc*. 81(6):1060–1067. https://doi.org/10.1016/J.MATPR.2021.04.379

Carne, R. H. R., A. A. Alade, B. O. Orji, A. Ibrahim, A. G. McDonald, and M. R. Maughan. 2023. A screw extrusion-based system for additive manufacturing of wood: Sodium silicate thermoset composites. *Adv. Mech. Eng*. 15(11):16878132231210373. https://doi.org/10.1177/16878132231210373

Chai, W., L. Zhang, W. Li, M. Zhang, J. Huang, and W. Zhang. 2021. Preparation of plastics- and foaming agent-free and porous bamboo charcoal based composites using sodium silicate as adhesives. *Materials* 14(10):2468. https://doi.org/10.3390/ma14102468

Ding, T., J. Xiao, S. Zou, and Y. Wang. 2020a. Hardened properties of layered 3D printed concrete with recycled sand. *Cem. Concr. Compos*. 113:103724. https://doi.org/10.1016/j.cemconcomp.2020.103724

Ding, T., J. Xiao, S. Zou, and X. Zhou. 2020b. Anisotropic behavior in bending of 3D printed concrete reinforced with fibers. *Compos. Struct*. 254:112808. https://doi.org/10.1016/j.compstruct.2020.112808

Ding, Y., Z. Pang, K. Lan, Y. Yao, G. Panzarasa, L. Xu, M. Lo Ricco, D. R. Rammer, J. Y. Zhu, M. Hu, X. Pan, T. Li, I. Burgert, and L. Hu. 2023. Emerging engineered wood for building applications. *Chem. Rev*. 123(5):1843–1888. https://doi.org/10.1021/acs.chemrev.2c00450

Feng, P., X. Meng, J.-F. Chen, and L. Ye. 2015. Mechanical properties of structures 3D printed with cementitious powders. *Constr. Build. Mater*. 93:486–497. https://doi.org/10.1016/j.conbuildmat.2015.05.132

Hegab, H., N. Khanna, N. Monib, and A. Salem. 2023. Design for sustainable additive manufacturing: A review. *Sustain. Mater. Technol*. 35:e00576. https://doi.org/10.1016/j.susmat.2023.e00576

Jaji, M. B., K. A. Ibrahim, G. P. A. G. van Zijl, and A. J. Babafemi. 2023. Effect of anisotropy on permeability index and water absorption of 3D printed metakaolin-based geopolymer concrete. *Mater. Today: Proc*. (in press). https://doi.org/10.1016/j.matpr.2023.06.394

Lai, L. W., and A. Idris. 2013. Disruption of oil palm trunks and fronds by microwave-alkali pretreatment. *BioResources* 8(2):2792–2804. https://doi.org/10.15376/biores.8.2.2792-2804

Novotný, M., K. Šuhajda, J. Sobotka, J. Gintar, and M. M. Eva Šuhajdova. 2014. Use of microwave radiation in building industry through application of wood element drying. *Wood Res-Slovakia* 59(3):389–400.

Orji, B. O., C. Thie, K. Baker, M. R. Maughan, and A. G. McDonald. 2023. Wood fiber–sodium silicate mixtures for additive manufacturing of composite materials. *Eur. J. Wood Wood Prod*. 81(1):45–58. https://doi.org/10.1007/s00107-022-01861-z

Pandey, K. K., and A. J. Pitman. 2003. FTIR studies of the changes in wood chemistry following decay by brown-rot and white-rot fungi. *Int. Biodeterior. Biodegradation* 52(3):151–160. https://doi.org/10.1016/S0964-8305(03)00052-0

Rasyid, M. F. A., M. S. Salim, M. R. Zakaria, H. M. Akil, Z. A. M. Ishak, and M. Z. A. Thirmizir. 2018. Effect of sodium silicate on the dimensional stability and mechanical behaviour of non-woven flax reinforced acrylic based polyester composites. *J. Mech. Eng.* 5(4):233–245.

Saroia, J., Y. Wang, Q. Wei, M. Lei, X. Li, Y. Guo, and K. Zhang. 2020. A review on 3D printed matrix polymer composites: Its potential and future challenges. *Int. J. Adv. Manuf. Technol*. 106(5):1695–1721. https://doi.org/10.1007/s00170-019-04534-z

Xiao, J., Z. Lv, Z. Duan, and S. Hou. 2022. Study on preparation and mechanical properties of 3D printed concrete with different aggregate combinations. *J. Build. Eng*. 51:104282. https://doi.org/10.1016/j.jobe.2022.104282

Xin, F. h., W. h. Liu, L. Song, and Y. Li. 2023. Research of compound additives on moisture resistance of sand cores bonded by sodium silicate. *Int. J. Metalcast*. 17(2):753–760. https://doi.org/10.1007/s40962-022-00805-w

Zahabizadeh, B., J. Pereira, C. Gonçalves, E. N. B. Pereira, and V. M. C. F. Cunha. 2021. Influence of the printing direction and age on the mechanical properties of 3D printed concrete. *Mater. Struct*. 54(2):73. https://doi.org/10.1617/s11527-021-01660-7